JOURNAL OF MATERIALS SCIENCE **40** (2005) 1625–1632

Ceramic flake formation in the aluminosilicate system by plasma spraying

J. G. FISHER*, K. CHANG, P. F. JAMES‡, P. F. MESSER, H. A. DAVIES
Department of Engineering Materials, University of Sheffield, Sir Robert Hadfield Building, Mappin Street, Sheffield S1 3JD, UK
E-mail: p.f.james@sheffield.ac.uk

Alumina and aluminosilicate flakes with compositions Al_2O_3, $3Al_2O_3{\cdot}2SiO_2$ and $Al_2O_3{\cdot}2SiO_2$ have been produced from commercial raw materials using a direct current plasma spray process in air. The microstructure and phase constitution of the as-sprayed flakes were examined with optical microscopy, scanning electron microscopy (SEM) and X-ray diffraction (XRD). Changes in phase constitution of the flakes with heat-treatment were examined using differential thermal analysis (DTA) and XRD of heat-treated samples. The as-sprayed Al_2O_3 flakes consisted of α-Al_2O_3 phase plus a minor γ-Al_2O_3 phase. The γ-phase could be removed by heat treating the flakes at 1300°C for 2 h. The aluminosilicate flakes consisted of $3Al_2O_3$:$2SiO_2$ (mullite) and an amorphous phase which crystallised to $3Al_2O_3$:$2SiO_2$ (mullite) after heat treatment at 1100°C for 2 h. These flakes may find applications as high temperature thermal insulation materials.

1. Introduction

Aluminosilicate fibres are commonly used in furnaces as insulating materials due to their strength retention at high temperatures, thermal shock resistance and low thermal conductivity. However, health and safety concerns over the use of fibres [1, 2] have prompted a search for alternative insulating materials. A possible replacement for aluminosilicate fibres are aluminosilicate flakes. In the present paper, plasma spraying was used to test the suitability of several aluminosilicate compositions for flake production. Previous plasma spraying work in the Al_2O_3-SiO_2 system has concentrated on the production of coatings or powders, with little attention having been given to the production of flakes.

Several workers have flame or plasma sprayed various forms of alumina to produce flakes, coatings and spheres [3–7]. Coatings had a laminar microstructure consisting of layers of flattened droplets. Metastable forms of alumina are often found in the sprayed products. More recently, Jiansirisomboon *et al.* have produced Al_2O_3/SiC nanocomposite coatings by plasma spraying sol-gel and freeze-dried powders [8]. Powders have been flame- and plasma sprayed in the Al_2O_3-SiO_2 system by a variety of methods [9–11]. Powders and coatings have been produced. Gani and McPherson produced Al_2O_3-SiO_2 sub-micron powders by injecting a mixture of Al_2Br_6 and $SiCl_4$ vapour into the tail flame of an oxygen-argon high-frequency plasma torch [10]. Depending on the Al_2O_3 content, the sprayed materials contained a mixture of amorphous phase, mullite and γ-Al_2O_3. Powders with Al_2O_3 contents $\leq$52 wt% formed amorphous materials. As the Al_2O_3 content of the powders increased (57–75 wt%) mullite and an amorphous phase appeared in the materials. For powders with 80–88.5 wt% Al_2O_3 content, mullite, γ-Al_2O_3 and an amorphous phase were present. Schmücker *et al.* plasma sprayed α-Al_2O_3/quartz admixtures corresponding to the stoichiometric mullite composition ($3Al_2O_3$:$2SiO_2$) [11]. Their sprayed materials consisted of an amorphous phase, residual α-Al_2O_3 and quartz, plus a small amount of mullite phase which crystallized from the melt. More recently, Khor and Li produced mullite/zirconia composite powders by plasma spraying a zircon/alumina mixture [12] and Chang *et al.* produced mullite/zirconia flakes using the same equipment as was used in the present work [13].

In this paper, work carried out on flake formation in the Al_2O_3-SiO_2 system by plasma spraying will be described. The objectives of the work were to use plasma spraying techniques to test the possibility of flake formation in the Al_2O_3-SiO_2 binary system and to study the microstructure and crystallisation behaviour of the flakes produced.

Current address: Department of Materials Science and Engineering, Korea Advanced Institute of Science and Technology, 373-1 Kusong-dong, Yusong-gu, Daejon 305-701, Korea.
‡Author to whom all correspondence should be addressed.

2. Experimental

The plasma spraying apparatus consists of a Sulzer Metco Type 9 MB arc plasma torch (Sulzer, Switzerland) mounted in a sound-proofed enclosure above a spinning copper wheel. Ceramic powders are fed into the plasma flame after it leaves the anode (serial feeding). The powder is melted and blown onto the wheel, where it deforms to produce flakes. These flakes are then thrown off the wheel and collected in a tray within the enclosure. A wire brush is fixed under the wheel to remove any material which adheres to it. After each run, the wheel was polished to remove any material that had not been removed by the brush. A schematic view of the plasma spraying apparatus can be found in [13].

The torch is powered by a three-phase transformer capable of operating at 500 A and 80 V. The plasma gas is an Ar/5–10% H_2 mixture. In the experiments a torch power of 40 kW was used. The powder feed rate was 10 g min^{-1} with each run lasting for 1 min. The torch—wheel distance was 135 mm.

The following compositions were chosen for spraying: Al_2O_3 (corundum), $3Al_2O_3{\cdot}2SiO_2$ (mullite) and $Al_2O_3{\cdot}2SiO_2$ (kaolin). Al_2O_3 and $3Al_2O_3{\cdot}2SiO_2$ are both already used in fibre form for thermal insulation. $Al_2O_3{\cdot}2SiO_2$ was chosen to test the flake forming ability of an aluminosilicate with a high SiO_2 content. The Al_2O_3 feed powder was a Baker Refractories coarse α-Al_2O_3 of diameter 63–90 μm. X-ray diffraction (XRD) of this powder showed it to consist entirely of α-Al_2O_3. The mullite feed powder was a Keith 73 sintered mullite of nominal composition 73 wt% Al_2O_3–25 wt% SiO_2 and diameter 63–80 μm. XRD of this powder showed it to consist of $3Al_2O_3{\cdot}2SiO_2$ mullite with α-Al_2O_3 present as a minor phase. The $Al_2O_3{\cdot}2SiO_2$ feed powder was an English China Clays Molochite powder of nominal composition 42 wt% Al_2O_3–55 wt% SiO_2 and diameter 63–90 μm. XRD of this powder showed it to consist of $3Al_2O_3{\cdot}2SiO_2$ (mullite) and an amorphous phase.

Sprayed powders were examined using transmission optical microscopy, scanning electron microscopy (SEM), differential thermal analysis (DTA) and X-ray diffraction. Both planar and cross-sectioned flake samples were studied by optical microscopy and SEM. Samples for XRD were sieved to remove unmelted particles and then ground to pass through a 45 μm sieve. Samples were analysed with a Phillips X-ray diffractometer using Co or Cu K_α radiation. Scans were carried out between 10–80° or 10–70° at 2° (2θ) min^{-1}, with a step size of 0.02°.

DTA was performed on crushed samples of sprayed mullite and kaolin powders using Pt crucibles with a heating rate of 10°C min^{-1} and a maximum temperature of 1100°C. Analysis was carried out in air. The extrapolated onset temperature of peaks was measured to determine phase change and crystallisation temperatures. Samples of alumina flakes were heat-treated at 1100 and 1300°C for 2 h. Samples of mullite and kaolin flakes were heat-treated at 1100°C for 2 h. Heat-treated samples were studied using XRD to determine the phases present.

TABLE I Flake dimensions and aspect ratios

Material	Flake length (μm)	Flake breadth (μm)	Aspect ratio (length/breadth)	Maximum flake thickness (μm)
Alumina	57–262 ± 7.5	46–177 ± 7.5	1–2.16	6–20 ± 1.0
Mullite	53–390 ± 5.0	39–290 ± 5.0	1–2.29	5–52 ± 2.5
Kaolin	72–310 ± 5.0	41–227 ± 5.0	1–3.62	25–63 ± 3.0

3. Results

Optical micrographs of the sprayed samples are shown in Fig. 1. The dimensions and aspect ratios of the flakes are given in Table I. Some of the alumina flakes consist of several particles of the starting powder which had splatted and adhered together, whilst others only consist of one particle (Fig. 1a). The mullite (Fig. 1b) and kaolin (Fig. 1c) flakes each consist of several particles of the starting powder which have melted, splatted and adhered together. Porosity is visible on the top and bottom surfaces of the flakes of all three compositions. Some unmelted and partially melted powder particles are also present in the samples. These unmelted and partially melted particles are more predominant in the mullite and kaolin samples than in the alumina sample.

SEM micrographs of the sprayed samples are shown in Fig. 2. Cross sections and side views of the flakes are shown in Fig. 3. The flakes consist of several powder particles that had splatted and adhered together to form a lamellae structure. Some of the particles in the flakes have only partially melted (marked with arrows). The flakes have very irregular surfaces. The top surfaces of the alumina flakes appear smoother than those of the mullite and kaolin flakes, suggesting that the molten alumina particles flowed more easily than the mullite and kaolin ones. This is to be expected, given the lower viscosity of alumina at high temperatures [14]. Cracking can be seen in some of the flakes. These are due to thermal stresses which form when the sprayed particles solidify [8]. Porosity is visible on the top and bottom sides of the flakes. Two types of porosity were visible: small circular closed pores, caused by gases trapped within the starting powder, and larger, irregularly shaped open pores, caused by the molten splats not flowing completely around each other.

DTA traces of the mullite and kaolin flakes are shown in Fig. 4. A DTA trace of a sprayed mullite sample is shown in Fig. 4a. A large exothermic peak can be seen at 954 ± 4°C. This peak is a mullite crystallisation peak. Similar peaks have been reported by several workers [9–11]. The sharpness and large size of the peak indicate that crystallisation occurred rapidly [15]. A DTA trace of a sprayed kaolin sample is shown in Fig. 4b. A sharp exothermic peak can be seen at 961 ± 4°C. This peak is due to crystallisation of mullite from the amorphous phase and is similar to the peak observed in the mullite flakes.

XRD traces of the flakes before and after heat treatment are shown in Fig. 5. The alumina flakes are shown in Fig. 5a. The untreated alumina flakes consist of α-Al_2O_3 with some γ-Al_2O_3 present as a minor phase. The flakes heat treated at 1100°C for 2 h show a

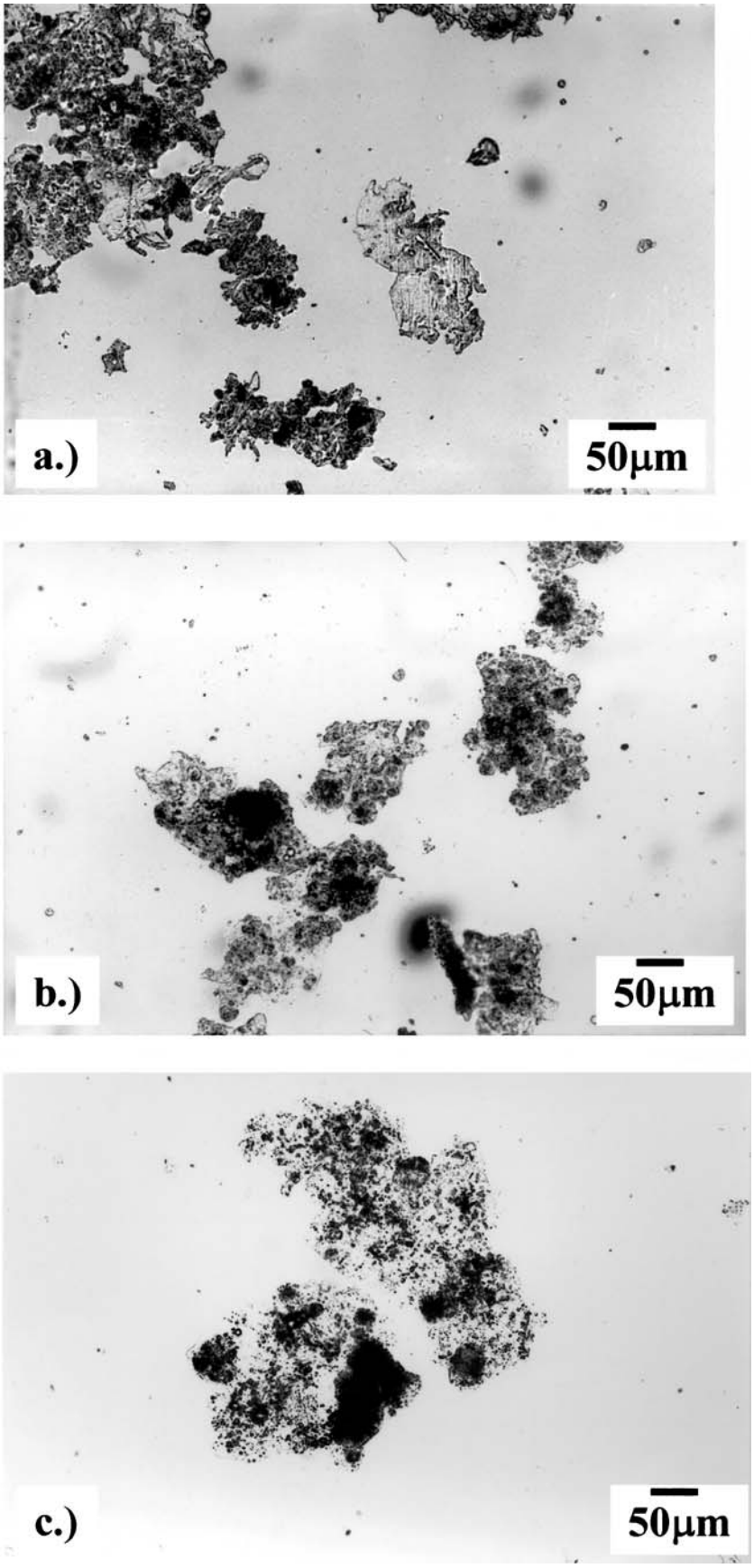

Figure 1 Optical micrographs of (a) sprayed alumina powder, (b) sprayed mullite powder, and (c) sprayed kaolin powder.

reduction in the intensity of the γ-Al_2O_3 peaks, indicating the conversion of γ-Al_2O_3 to α-Al_2O_3. The flakes have converted entirely to α-Al_2O_3 after heat treatment at 1300°C for 2 h. An unknown phase is also present in the samples heat treated at 1100 and 1300°C for 2 h. The XRD traces do not show evidence of conversion of the γ-Al_2O_3 to the intermediate δ- or θ-phases before conversion to the stable α-Al_2O_3 phase.

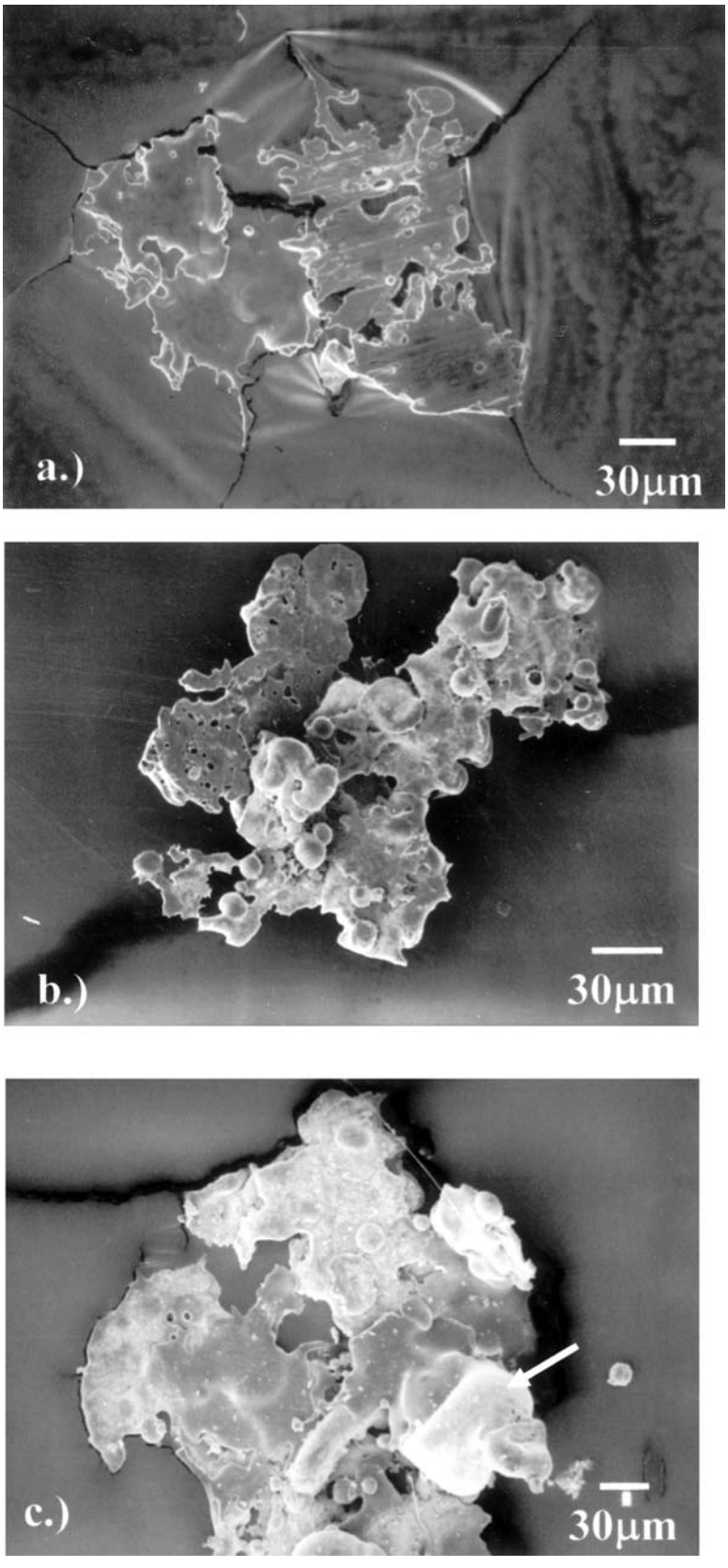

Figure 2 SEM micrographs of (a) sprayed alumina powder, (b) sprayed mullite powder, and (c) sprayed kaolin powder.

XRD traces of a sprayed mullite sample before and after heat-treatment at 1100°C for 2 h are shown in Fig. 5b. The sprayed sample before heat-treatment consisted of mullite with α-Al_2O_3 present as a minor phase. A "hump" can be seen between 20° and 40°, indicating that an amorphous phase is also present. This amorphous hump was no longer present in the heat-treated sample, indicating that the sample had completely crystallised. The heat-treated sample had crystallised to mullite, with α-Al_2O_3 present as a minor phase. The temperature of heat-treatment was too low to cause any significant reaction of the α-Al_2O_3 with the surrounding mullite.

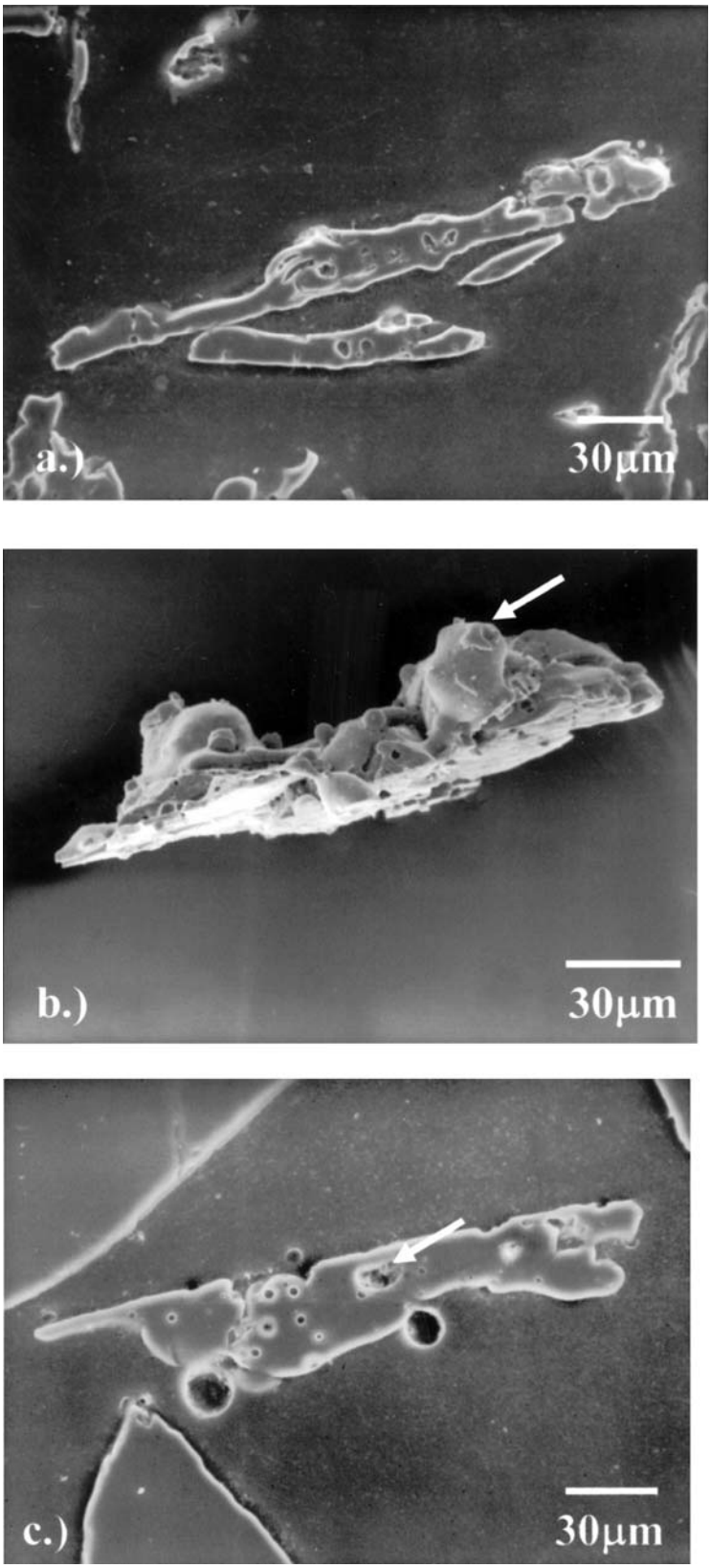

Figure 3 (a) Cross section of alumina flakes, (b) side view of mullite flake, and (c) cross section of kaolin flake.

XRD traces of a sprayed kaolin sample before and after heat-treatment at 1100°C for 2 h are shown in Fig. 5c. The sprayed sample before heat-treatment consisted almost entirely of an amorphous phase, with mullite remaining as a minor phase. The size of the amorphous peak in the heat-treated sample is reduced, although still present. $3Al_2O_3{\cdot}2SiO_2$ (mullite) crystallised in the heat-treated sample.

4. Discussion

From the optical and scanning electron micrographs, it can be seen that the alumina flakes consisted mostly of several droplets which have splatted and adhered together. The morphology of the flakes is similar to that of the single alumina splats produced by Vardelle and Besson [7]. Like their single splats, the alumina flakes contain spherical and elongated porosity, and

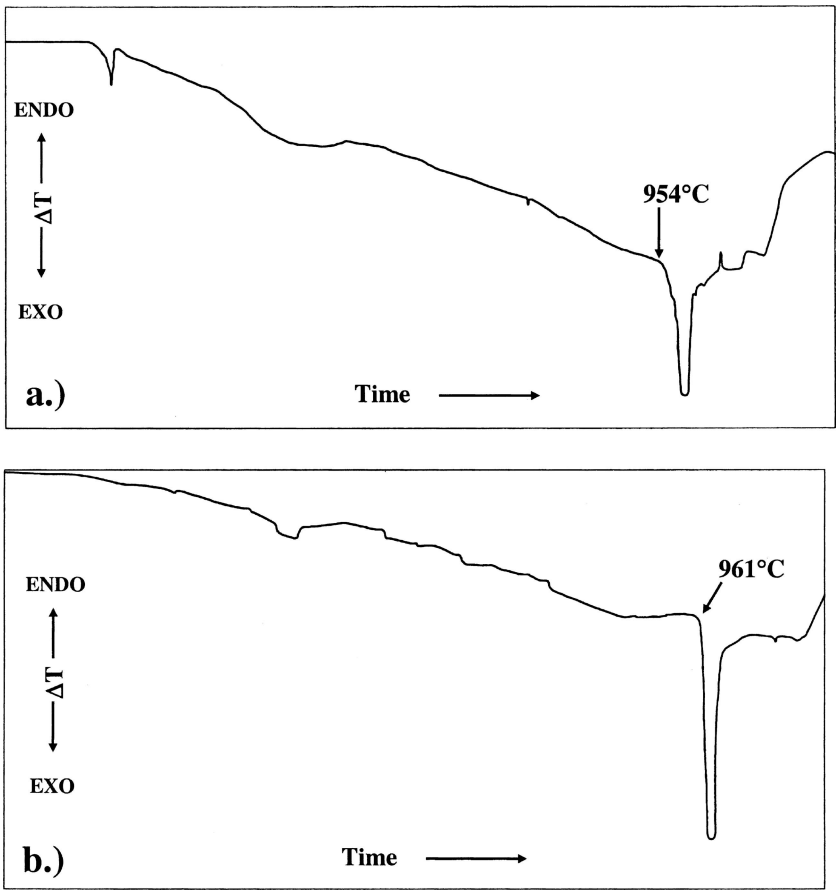

Figure 4 Differential Thermal Analysis traces of (a) mullite flakes and (b) kaolin flakes.

microcracking due to thermal gradients in the flakes. The irregular edges of the flakes indicate that the edges of the splats broke up into small droplets upon impact with the wheel.

The alumina flakes produced in this study differed from the flame and plasma-sprayed materials produced by other workers in that they consist mainly of α-Al_2O_3 while the materials produced by other workers consisted mainly of transition aluminas such as δ-Al_2O_3, γ-Al_2O_3 and θ-Al_2O_3. Scanning electron microscopy of the flakes showed that some flakes contain partially melted particles. If the particles have not completely melted, they would contain α-Al_2O_3 cores which would act as nucleation sites during recrystalisation [16]. The splats would then solidify as α-Al_2O_3. The presence of γ-Al_2O_3 in the flakes would be due to particles which had melted completely and which had sufficient undercooling on solidification to crystallise in a metastable form.

The mullite flakes are similar in morphology to the alumina flakes. It can be seen from the optical and scanning electron micrographs that the mullite flakes consisted of several layers of particles which have melted, splatted and bonded together. The irregular edges of the flakes indicate that the edges of the splats broke up into small droplets upon impact with the wheel. From the scanning electron micrographs, it can be seen that the mullite and kaolin flakes had small spherical particles attached to the top surface of the flakes. These spheres have originated from small secondary particles present in the starting material. These particles will have melted but not splatted upon impact with previous splats. This has previously been observed in alumina coatings and was attributed to the increase in surface tension of the particles as their diameter decreases [7]. The mullite/zirconia composite flakes produced by Chang *et al.* [13] are very similar in morphology to the ones in this study, consisting of layers of splats, some unmelted particles and spherical and elongated porosity. In addition, their flakes contained ZrO_2 particles distributed throughout the flakes.

X-ray diffraction of the mullite flakes showed them to consist of a $3Al_2O_3$:$2SiO_2$ mullite phase, an α-Al_2O_3 phase and an amorphous phase. The mullite phase is due to particles in the flakes which did not melt completely. The α-Al_2O_3 present in the flakes is unreacted alumina from the starting powder. The amorphous phase is caused by molten particles cooling quickly enough to avoid devitrification. Gani and McPherson produced powders of similar composition (63.8 mol% Al_2O_3 −36.2 mol% SiO_2) which consisted of mullite and amorphous phase [10]. Their powders were produced by passing mixed halide gases through an argon-oxygen plasma flame. The halide compounds would have oxidized, condensed to form liquid droplets and then solidified so the mullite phase present in their powders would have crystallized during cooling. Khor and Li produced partially amorphous mullite/zirconia composite powders by plasma spraying alumina/zircon mixtures [12]. The mullite phase present in their powders would have crystallised from the melt during cooling. The mullite/zirconia flakes produced by Chang *et al.* consisted

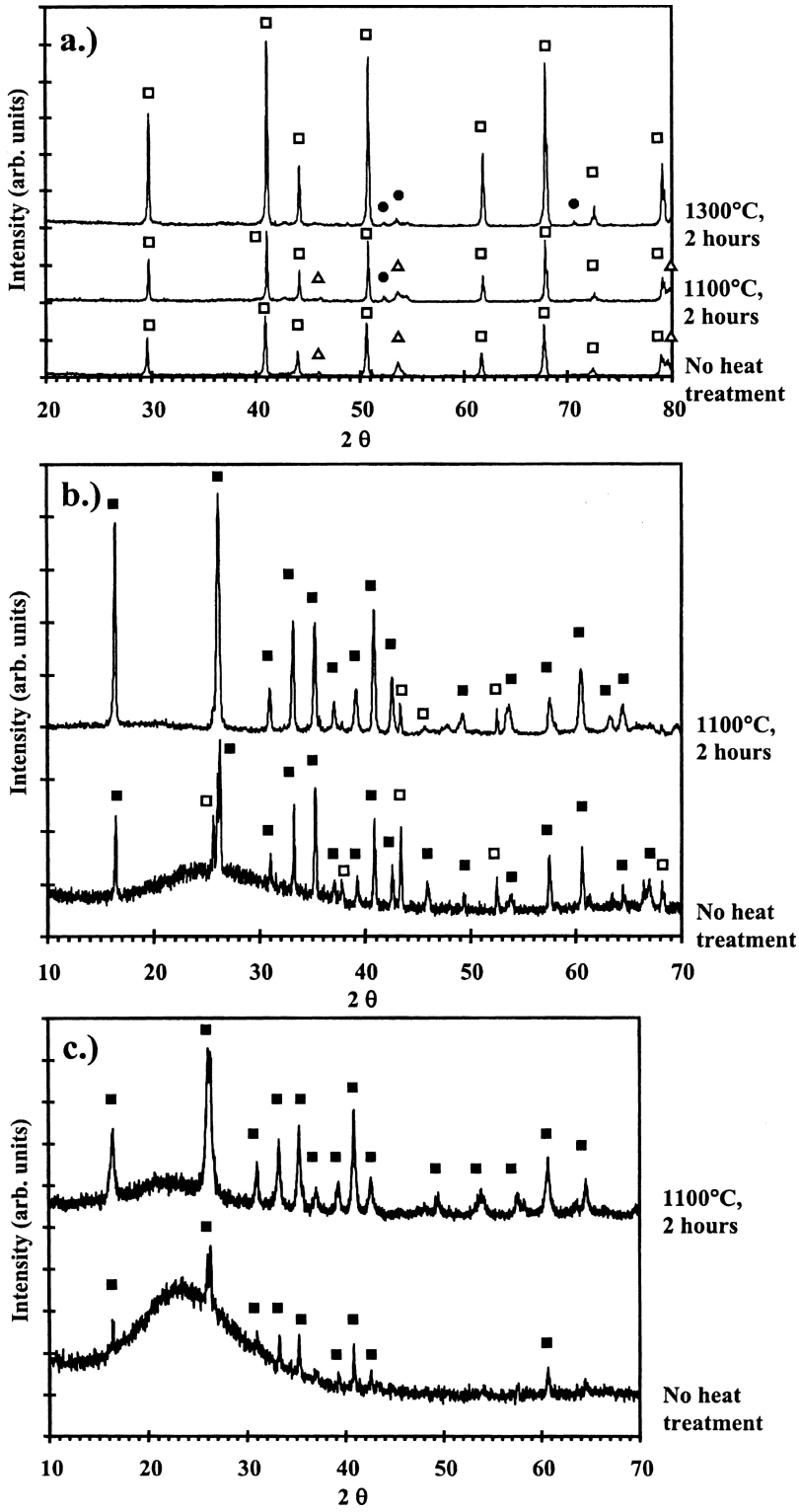

Figure 5 X-ray Diffraction traces of (a) alumina, (b) mullite, and (c) kaolin flakes. □ = α-Al_2O_3; △ = γ-Al_2O_3; ● = unknown phase; ■ = Mullite 3 Al_2O_3·2SiO_2.

of an amorphous phase, mullite and zirconia [13]. In the present work, the mullite phase is due to incomplete melting of the sprayed powder.

X-ray diffraction of the unsprayed kaolin powder showed it to consist of $3Al_2O_3$:$2SiO_2$ mullite and an amorphous phase. In the sprayed kaolin flakes, X-ray diffraction showed that the mullite phase had almost disappeared. The cooling rate of the splats during solidification was sufficient to suppress crystallisation of mullite from the molten particles. Gani and McPherson produced amorphous Al_2O_3-SiO_2 powders of this composition [10]. Again, their powders were produced by condensation from liquid droplets and cooled rapidly enough to avoid crystallisation of mullite. In our work, SEM of the flakes showed that partially melted particles were present in some of the flakes. Therefore the residual mullite phase present in the X-ray trace of the flakes is due to particles that did not melt completely during their passage through the plasma flame.

XRD results of the heat treated alumina flakes show that the γ-Al_2O_3 within the flakes is converted entirely to α-Al_2O_3 within the temperature range 1100–1300°C, as found by Ault [5]. The absence of transition aluminas is unusual. It is possible that the amounts of δ- or θ-phase in the flakes are too low to be detected by XRD.

DTA results for the mullite and kaolin flakes show that they crystallised at temperatures within 10–15°C of each other, in the range 950–965°C. Both types of flake exhibited large crystallisation peaks, indicating rapid crystallisation. Such crystallisation peaks are often found in the DTA traces of binary silicate glasses [15]. The mullite and kaolin flakes from this work crystallised at lower temperatures (20–40°C lower) than Al_2O_3-SiO_2 glasses of the corresponding compositions in references [9–11]. However their crystallisation temperatures are similar to those of polymeric Al_2O_3-SiO_2 xerogels [17] and of commercial Al_2O_3-SiO_2 glass fibres [18]. Differences in crystallisation temperature may be due to different heating rates used in the DTA experiments. XRD results show that mullite crystallised directly from the amorphous phase as has been found in glasses [18] and monophasic gels [17]. Unlike the mullite/zirconia composite powders produced by Khor and Li, spinel was not formed during heat treatment of the flakes in the present work [12]. Spinel was also not formed during heat treatment of the mullite/zirconia flakes produced by Chang *et al.* [13]. Rather, mullite crystallised directly from the amorphous phase.

It was found that as the SiO_2 content of the starting powder increased, the amount of unmelted and partially melted material present in the sprayed powder increased, and the amount of flakes decreased. Addition of SiO_2 causes a decrease in thermal conductivity. The thermal conductivity of Al_2O_3 at 1400°C is 0.054 $Wcm^{-1}K^{-1}$ whereas the thermal conductivity of mullite at 1400°C is 0.038 $Wcm^{-1}K^{-1}$ [19]. The decrease in thermal conductivity will make melting of the mullite and kaolin powders more difficult, even though their melting points are lower than that of Al_2O_3 [20]. Therefore flake formation was less efficient when mullite and kaolin powders were sprayed.

5. Conclusions

Plasma spraying has been successfully used to test the possibility of flake formation in the Al_2O_3-SiO_2 system. Flakes with compositions of Al_2O_3, $3Al_2O_3{\cdot}2SiO_2$ (mullite) and $Al_2O_3{\cdot}2SiO_2$ (kaolin) were produced.

Some of the alumina flakes consisted of single droplets which had splatted, whilst others consisted of several droplets which had impacted onto the wheel or previously sprayed material, splatted and adhered together. The mullite and kaolin flakes consisted of several droplets which had impacted onto the wheel or previously sprayed material, splatted and adhered together. Porosity and microcracking was present within flakes from all three compositions.

The Al_2O_3 flakes consisted predominantly of the stable α-Al_2O_3 phase plus some metastable γ-Al_2O_3 phase formed by the rapid quenching of the molten droplets. The γ- phase could be removed by heat treating the flakes at 1300°C for 2 h. The mullite and kaolin flakes consisted of $3Al_2O_3$:$2SiO_2$ (mullite) and an amorphous phase. The amorphous phase in both mullite and kaolin flakes crystallised to $3Al_2O_3$:$2SiO_2$ (mullite) after heat treatment at 1100°C for 2 h. The mullite flakes could by completely crystallized by heat-treatment, but the kaolin flakes retained some amorphous phase.

Acknowledgements

This work was supported by grants from the UK Department of Trade and Industry, the Engineering and Physical Sciences Research Council LINK programme, and Morgan Materials Technology Ltd. The authors would like to thank T. Eaton and P. Staton for operating the plasma spray equipment and G. Jubb (Thermal Materials UK) for comments on the paper.

References

1. I. C. ALEXANDER, G. A. JUBB and J. A. PENN, *Brit. Ceram. Trans.* **96**(2) (1997) 74.
2. ECFIA Action, "European Ceramic Fibre Industries Association," # Rue de Colonel Moll, 75017 Paris, France, Information Sheets Nos. 2 and 3, March 1999.
3. M. PLUMMER, *J. Appl. Chem.* **8**(1) (1958) 35.
4. T. I. BARRY, R. K. BAYLISS and L. A. LAY, *J. Mat. Sci.* **3** (1968) 229.
5. N. N. AULT, *J. Am. Ceram. Soc.* **40**(3) (1957) 69.
6. J. B. HUFFADINE and A. G. THOMAS, *Powder Metall.* **7**(14) (1964) 290.
7. M. VARDELLE and J. L. BESSON, *Ceram. Intern.* **7**(2) (1981) 48.
8. S. JIANSIRISOMBOON, K. J. D. MACKENZIE, S. G. ROBERTS and P. S. GRANT, *J. Eur. Ceram. Soc.* **23** (2003) 961.
9. T. TAKAMORI and R. ROY, *J. Am. Ceram. Soc.* **56**(12) (1973) 639.
10. M. S. J. GANI and R. MCPHERSON, *J. Mat. Sci.* **12** (1977) 999.
11. M. SCHMÜCKER, H. SCHNEIDER, M. POORTEMAN, F. CAMBIER and R. MEINHOLD, *J. Eur. Ceram. Soc.* **15** (1995) 1201.
12. K. A. KHOR and Y. LI, *Matt. Lett.* **48** (2001) 57.
13. K. CHANG, H. R. REZAIE, I. C. ALEXANDER, H. A. DAVIES, P. F. MESSER and P. F. JAMES, *J. Non-Cryst. Sol.* **290** (2001) 231.
14. G. URBAIN, Y. BOTTINGA and P. RICHET, *Gochimica et Cosmochimica Acta* **46** (1982) 1061.
15. F. W. WILBURN and J. B. DAWSON, in "Differential Thermal Analysis Volume 2: Applications," edited by R. C. Mackenzie, (Academic Press, London and New York, 1972) p. 238.
16. R. MCPHERSON, *J. Mat. Sci.* **15** (1980) 3141.
17. K. OKADA, J. KANEDA, Y. KAMESHIMA, A. YASUMORI and T. TAKEI, *Matt. Lett.* **57** (2003) 3155.
18. T. TAKEI, Y. KAMESHIMA, A. YASUMORI and K. OKADA, *J. Am. Ceram. Soc.* **82**(10) (1999) 2876.
19. J. F. SHACKELFORD, W. ALEXANDER and J. S. PARK, in "CRC Materials Science and Engineering Handbook," 2nd ed. (CRC Press, Boca Raton, 1994) p. 278.
20. I. A. ASKAY and J. A. PASK, *J. Am. Ceram. Soc.* **58** (1975) 507.

Received 20 February
and accepted 8 November 2004